AIAA 81-0142R

Flight Performance and Drift Minimization of Magsat in the Lower Atmosphere

Ramasamy G. Sellappan*
RCA American Communications, Inc., Princeton, N.J.
and
Ashok K. Saxena†
Fairchild Space and Electronics Company, Germantown, Md.

This paper addresses the dynamic characteristics of a momentum biased spacecraft (Magsat) which was placed in an elliptic, sun synchronous, low Earth orbit. It discusses various dynamic phenomena observed, develops models for their plausible explanation, and suggests techniques for preventing or minimizing adverse phenomena. An aerodynamic coefficient model which accounts for atmospheric super-rotation is proposed. This model is used to conduct analysis and simulations, the results of which are shown to be compatible with data taken by Magsat. A control philosophy is developed, and analytic expressions for the long-term motion of the momentum biased axis for special cases are derived.

Introduction

OPERATIONAL experience and analysis of the long-term attitude drift of spacecraft in low Earth orbit has received relatively little attention in recent years. One reason for this may be the presence of active control systems on spacecraft in this flight regime which tend to reduce the observability of various environmental and dynamic phenomena. The emphasis on such topics is likely to change in the near future with the advent of the shuttle era in which the use of inexpensive free fliers is emphasized.

Earlier work of this nature has been principally limited to the Atmospheric Explorer and the Skylab spacecraft. Nurre[1] investigated the effect of perturbing aerodynamic torques on a gravity gradient stabilized spacecraft. This was the orientation in which Skylab was placed in 1974 after the final mission was completed. Sperling[2] examined the effects of aerodynamic and gravity gradient torques on a Skylab type of spacecraft. Nurre and Sperling represented the aerodynamic torque by a Fourier series. Meirovitch[3] applied Liapunov's method to determine equilibrium criteria for a spacecraft subjected to aerodynamic and gravity gradient torques. In this approach, the aerodynamic torque was derived from a potential function. Recently Buchanan et al.[4] determined equilibrium positions and bounds on the motion of the spin axis. They also presented simulation results and compared them with data telemetered from Skylab. This work addresses the dynamics of a momentum biased spacecraft in the lower atmosphere where the effect of aerodynamics is significant. The emphasis is on understanding the qualitative nature of the dynamics rather than the precise matching of telemetered data with simulation results.

This work was motivated by the seven-month Magsat mission. The spacecraft was placed into an elliptical sun synchronous orbit in Oct. 1979. This mission demonstrated the need and importance of understanding environmental torques and drift characteristics in low altitude flight. Magsat was a momentum biased spacecraft on which control torques were generated by magnetic coils. Since the primary objective of the mission was to map the geomagnetic field whose measurement was corrupted by the activation of control coils, it was desirable to develop and refine during flight, a control strategy that would minimize the application of control torques. The results of this work include expressions for the preferred orientation of a momentum biased spacecraft in a circular orbit and for the frequency of the long-term motion. This in turn suggests how such a spacecraft with aerodynamic control surfaces may be designed so that the normal to the momentum vector will point at various, though controllable, off-nadir orientations. If the initial orientation is away from this preferred orientation, a scanning motion, whose frequency and direction can be controlled by varying the aerodynamic control surface, may be generated.

Background

Spacecraft Description

The spacecraft consisted of a base module to which were attached four solar panels and an experiment module. The total spacecraft weight was 179.88 kg. It was 1.55 m in height, and with the solar panels extended in the orbit configuration, the tip-to-tip dimension was 3.4 m (Ref. 5). Figure 1 shows its breakdown into base and instrument modules with the boom supporting the magnetometer platform containing vector and scalar magnetometers and a precision sun sensor. The base module housed the power, telemetry, command, Doppler-tracking, tape recorders, and attitude control systems. The instrument module contained an optical bench, star cameras, and a precision attitude transfer system optically linking the star cameras to the magnetometer sensor platform.

The spacecraft was three-axis stabilized with the magnetometer boom trailing aft. The roll-yaw control system was designed to maintain alignment of the pitch-axis near the negative orbit normal by using a momentum biased IR scanner/reaction wheel, magnetic torquing for initial orientation and occasional control with a microprocessor, and semiautonomous control logic.[6] The roll output of the IR scanner could be used to determine the difference in right ascension between the pitch axis and the negative orbit normal (NON) when the spacecraft was near the equator. Since the spacecraft was in a near-polar orbit, this output at the poles provided the difference between the declinations of the pitch axis and the NON. These errors could be corrected by using a pitch axis magnetic dipole at appropriate places in the orbit. The activation of the pitch coil could be minimized by uplinking an acceptable upper bound on the errors.

Presented as Paper 81-0142 at the AAS/AIAA Astrodynamics Specialist Conference, Lake Tahoe, Nev., Aug. 3-5, 1981; submitted Dec. 9, 1981; revision received May 13, 1982.

*Principal Member of Engineering Staff, Spacecraft Engineering Department. Member AIAA.

†Staff Engineer, Space Products Directorate. Member AIAA.

In order to provide a slow smooth response, the pitch loop during the mission mode was overdamped and had a low bandwidth. The IR scanner provided pitch angle feedback while a gyro provided the pitch rate feedback for damping purposes. If the wheel speed exceeded a commanded threshold, momentum dumping was exercised automatically by activation of magnetic coils. The secular buildup of angular momentum due to aerodynamic and gravity gradient torques was minimized by uplinking a pitch bias angle to the spacecraft.

Prelaunch analysis[6] had indicated that at Magsat's low operating altitudes, aerodynamic torques would cause the major attitude disturbance. Roll aerodynamic torques were considered to be essentially nonexistent due to spacecraft symmetry. The pitch aerodynamic torques were stabilizing due to the trailing boom, whereas the yaw aerodynamic torques were unbalanced. Uncertainties in aerodynamic shadowing, gas-surface interactions, and the spacecraft mass center precluded the use of a fixed aerodynamic trim surface. The final design incorporated a 1.3-cm-diam interlocking boom that could be extended/retracted in flight. The boom was mounted along the negative pitch axis and could be extended to a maximum length of 12 m.

In-Flight Performance

Magsat was launched on Oct. 30, 1979. The initial orbit had an inclination of 97 deg with the perigee and apogee heights being 350 and 560 km, respectively. From a dynamicist's viewpoint, the mission life span can be divided into three periods. The first period lasted about three weeks during which the attitude was acquired and trimmed.[7] The experiment boom was deployed and the trim boomlength was adjusted for satisfactory performance. The second period, which lasted for four and one half months, can be considered to be the nominal mission phase. Since the mission was designed to last five months and orbit decay was slower than expected, the final two months of the mission were such that the sun angle was not favorable and there were longer periods of darkness. This resulted in both power and thermal complications. During this period the spacecraft was targeted to a non-nominal attitude in an effort to improve spacecraft health. This resulted in considerable drift and magnetic torquing. Tape recorders were turned off to save power and so attitude data was sparse during these periods.

As discussed earlier, the spacecraft was intentionally biased in pitch to minimize the secular buildup of angular momentum about the pitch axis. During the first few months, this angle was small, positive, and did not appear to change much. Stengle[7] indicates that there appeared to be some correlation between the sunspot cycles and the changes in the pitch angle; i.e., there was some correlation between density and the equilibrium pitch position. There was a period of about two weeks which occurred six and one half months into the mission during which there was apparently no pitch angle for which the spacecraft was in equilibrium or near equilibrium. At the onset of this period, the spacecraft had to be pitched positively to about 8 deg. Subsequently the pitch equilibrium angle had a large negative value after which it reduced in magnitude. One of the objectives of this work was to determine if an analytic method could be employed to explain this behavior.

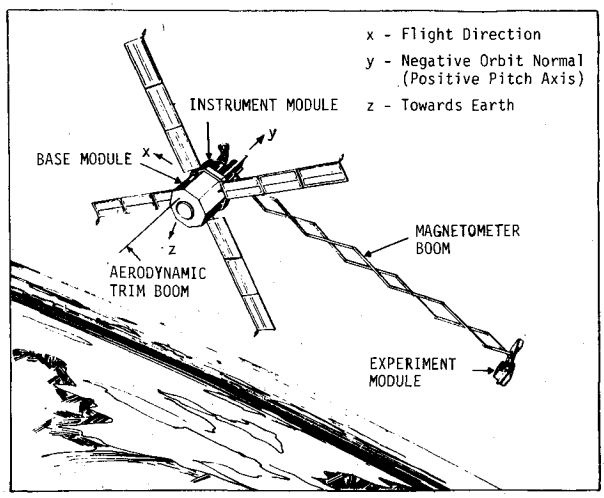

Fig. 1 Artist's conception of Magsat.[7]

The primary objective was to provide a better understanding of the roll-yaw dynamics of the spacecraft with different lengths of the aerodynamic trim boom. This motion is defined by the motion of the point of intersection of the spacecraft pitch axis ($+y$) axis and the celestial sphere, as it appears to an observer located outside the celestial sphere along the $+y$ direction. The pitch axis was observed to drift in a clockwise sense over the period of one orbit. Sometimes the pitch axis appeared to undergo a periodic motion about a point about 5 deg above NON. This motion was counterclockwise in direction and its period was of the order of five days. During the early portion of the mission there was some indication that this point itself may be moving with a period of few weeks. Prelaunch simulations conducted by Tossman[6] had indicated that the motion of the pitch axis over long periods of time was generally counterclockwise and about a point about 4 deg above NON. It appeared as if the tendency for the pitch axis to stay about 4 deg above NON was due to the spacecraft's tendency to fly into the relative wind. The current work was motivated by the desire to obtain further insight by using an analytic approach. In particular, it was desirable to determine how the aerodynamic trim boom could be adjusted so that drift could be minimized over extended periods of time. It was desirable to show that the motion occurred about a point (trim point) above the NON and that it was always in the counterclockwise sense. It was also desirable to support the observation that the arc length traversed across the celestial sphere by the pitch axis was greater if the initial attitude was further from the trim point.

Technical Approach

The approach used in this paper is to develop an aerodynamic torque model which is mathematically sound and analytically tractable. The general equations of motion for a spacecraft having products of inertia and placed in an elliptic orbit are derived. They are linearized about the nominal attitude and rates. The condition under which secular buildup of angular momentum about the pitch axis can be minimized is determined by an integral approach. The time histories of this pitch angle and the pitch bias uplinked to the spacecraft are shown to be in good agreement. By approximating the linearized equations of the motion, closed form solutions are obtained for circular orbits. A coordinate transform is used to express the roll-yaw solution in terms of right ascension and declination angles relative to the NON. This provides insight to the problem of drift minimization and potential control philosophies for momentum biased spacecraft in the lower atmosphere. Telemetered data and the results of simulations are used to validate the aerodynamic model, and to support the proposed control philosophy.

Aerodynamics

Thermosphere Model

The model used in this work assumes the atmosphere to be axially symmetric in zonal winds and spherically symmetric in density. The atmospheric winds are assumed to be purely zonal. First-order meridional components are not included as zonal effects are known to dominate. King-Hele's model[8] is used to depict the variation in the atmospheric rotation rate as

a function of altitude. This model was determined from data taken by several satellites and indicates that super-rotation of the atmosphere occurs at altitudes below 413 km with the peak being at about 367 km. The model[8] can be approximated by the following piecewise linear function.

$$\begin{aligned}\omega_a &= 2.2617 - 0.0031\,h, && 413 < h \le 560\\ &= 4.5713 - 0.0087\,h, && 367 < h \le 413\\ &= 0.8311 + 0.0015\,h, && h \le 367\end{aligned} \tag{1}$$

The atmospheric rotation rate ω_a is in revolutions/day and the altitude h is in km.

Since the emphasis of this study was in a qualitative understanding of the dynamics, the variation in the density due to many environmental effects such as geomagnetic storms and solar flares was not factored into this study. The density variation is based on Jacchia's model[9] and is expressed by the equation

$$\rho(h) = k\exp(-h/62)\ \text{kg/m}^3 \tag{2}$$

The exospheric temperature was assumed to be in the range of 1200-1300 K. This corresponds to a period of high solar activity. For this period, the constant k had a value of 5.293×10^{-9}.

Aerodynamic Coefficient Model for Aerodynamic Torque

Aerodynamic data on Magsat was available in the form of a model which decomposed the spacecraft into small elements. In this flight regime the mean-free path between molecules is much greater than the spacecraft dimension. The drag force F_i acting on a surface element of area A_i is given by the expression

$$F_i = -\rho V_d^2 A_i[(2-\sigma_n-\sigma_t)(\bar{e}_{ni}\cdot\bar{e}_v)^2\bar{e}_{ni} + \sigma_t(\bar{e}_{ni}\cdot\bar{e}_v)\bar{e}_v] \tag{3}$$

Here, V_d is the magnitude of the wind vector, σ_t the tangential momentum exchange coefficient ($\simeq 0.9$), θ the normal momentum exchange coefficient ($\simeq 0.9$), $\bar{e}_{ni}$ the unit vector pointing normally outward from the surface A_i, and $\bar{e}_v$ the unit wind vector entering the surface areas. Knowing the location of the center of mass of the spacecraft and the center of pressure of each surface element, the aerodynamic torque can be computed. This formulation is convenient for simulation purposes. In order to make the problem analytically tractable, another model is derived from the given model.

The approach used is to heuristically postulate the structure of the model and then show that values of parameters can be derived within the structure so that the computed torques are close to those obtained from the decomposition model. For Magsat, a model structure is proposed so that the total aerodynamic torque can be separated into a torque which depends only on the trim boom length and a torque which depends only on the attitude state of the spacecraft.

The total aerodynamic torque T_a is, thus, given by the expression

$$T_a = P_d[N_B(L) + N_A(\tilde{\tilde{\Phi}})]; \qquad P_d = \tfrac{1}{2}\rho V_d^2 \tag{4}$$

Here, L is the length of the trim boom in meters, and $\tilde{\tilde{\Phi}}$ the state vector representing the orientation of the body reference from with respect to the wind reference frame. The reference frames will be defined in a sequel. At this time, attention is focused on the model structure which suggests that the aerodynamic torque can be represented by the Taylor's series

$$T_a = P_d[N_0 + \tilde{\tilde{N}}_L L + N_L L^2 + \sigma^3 + N_J\tilde{\tilde{\Phi}} + \sigma_A^2] \tag{5}$$

$$n_{Jik} = \left(\frac{1}{P_d}\right)\left[\frac{\partial T_{ai}}{\partial\tilde{\tilde{\Phi}}_k}\right]_{\tilde{\tilde{\Phi}}=0} \tag{6}$$

where σ^3 is the third- and higher-order terms containing L, and σ_A^2 the second- and higher-order partial derivative terms. N_0 is the bias torque with the boom fully retracted. Since both the aerodynamic force on the boom and its moment arm vary linearly with boom length, N_L is sufficient to describe the boom length, N_L is sufficient to describe the boom length dependency. It will be shown that the aerodynamic characteristics of Magsat can be approximated by neglecting σ_A^2 for small angles $\tilde{\tilde{\Phi}}$. The aerodynamic torque is, thus, expressed by the relation

$$T_a = P_d[N_0 + N_L L^2 + N_J\tilde{\tilde{\Phi}}] \tag{7}$$

The aerodynamic characteristics of Magsat were generated from the decomposition model. Figures 2 and 3 show the effect of changing the pitch and yaw angles on the aerodynamic pitch and yaw torques. The density ρ and the velocity V_d used to generate these figures were 1.0×10^{-11} kg/m^3 and 7700 m/s, respectively. The figures suggest that it may be possible to approximate the decomposition model by the proposed model structure. Details of this justification including the numerical values for the partial derivatives can be found in Ref. 10. The numerical values of the aerodynamic parameters are given by the following equations.

$$N_0 = [0.0 \quad 2.6490\times10^{-3} \quad 0.7593]^T \ \text{m}^3 \tag{8}$$

$$N_L = [0.0 \quad 0.0 - 0.0156]^T \ \text{m} \tag{9}$$

$$N_J = \begin{bmatrix} 0.0 & -0.1249 & 0.0024 \\ 0.0 & -0.9354 & 0.0042 \\ 0.0 & 0.0094 & -0.8827 \end{bmatrix} \text{m}^3/\text{rad} \tag{10}$$

In order to complete the discussion on the aerodynamic model, it remains to define the vector $\tilde{\tilde{\Phi}}$. This can be done by defining the attitude and wind reference frames. The z axis of the attitude reference frame is directed toward the geocenter and the y axis points along the NON. The direction of the x axis is such that it completes a right-handed system of axes. The body reference frame is obtained by a series of three

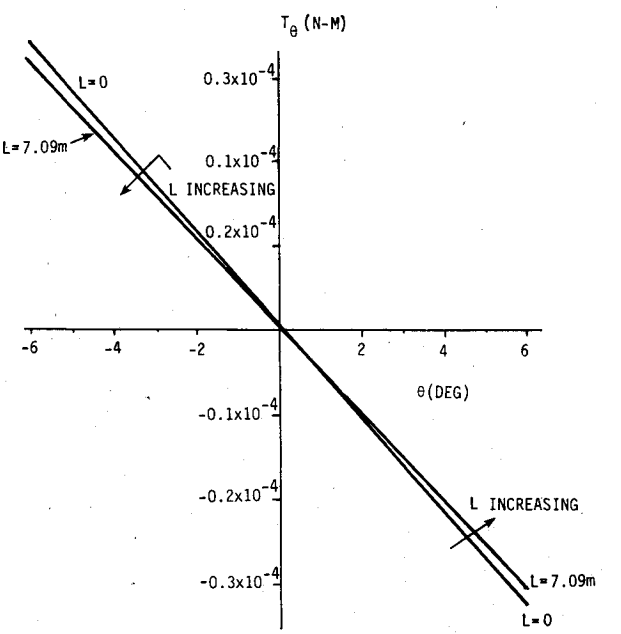

Fig. 2 Pitch aerodynamic torque vs pitch angle for different boom lengths.

rotations from the attitude reference frame. These are given by a rotation through an angle ψ about the z axis, a rotation through an angle ϕ about the x axis, and a rotation through an angle θ about the y axis. The attitude of the spacecraft is, thus, defined by the state vector Φ

$$\Phi = [\phi \quad \theta \quad \psi]^T \tag{11}$$

The wind reference frame is such that the x axis points directly into the relative wind, the z axis points toward the geocenter, and the direction of the y axis is such that the system forms a right-handed triad. The attitude reference frame can be obtained by a series of small rotations ψ^*, ϕ^*, and θ^* from the wind reference frame. For small attitude angles, $\tilde{\Phi}$ is given by the relation

$$\tilde{\Phi} = \Phi + \Phi^* \tag{12}$$

The aerodynamic model used for this work, thus, can be defined by Eqs. (4), (7), and (12).

Expressions for the wind circulation in the atmosphere, and the radial and tangential components of the spacecraft velocity can be used to establish the following relationships:

$$\theta^* = -e\sin f/(1+e\cos f) \tag{13}$$

$$\psi^* = [(\omega_a/\omega_0)\sin i]\,(1-2e\cos f)\cos(D+f) \tag{14}$$

Here f is the true anomaly, ω_0 the mean orbital rate, and D the argument of perigee.

Equation (14) holds for small values of eccentricity e. Note that the first column of N_J is zero for Magsat and so that the value of $\tilde{\phi}$ is not important for computing the aerodynamic torque. Equation (14) shows that the maximum effect of the atmospheric winds occurs at the nodes and that this rotation induced angle is positive at the ascending node. The variation in ψ^* is not harmonic even to the first order in eccentricity. For circular orbits it can be shown that at an altitude of 350 km, this angle is 7.03% greater than the angle induced at an altitude of 300 km. Hence, for circular orbits in this height regime, the angle ψ^* decreases over the mission.

Pitch Axis Results

One of the objectives of this work was to obtain a better understanding of the pitch bias history. In particular, it was important to identify the time period during which there was no pitch angle at which the spacecraft was in equilibrium or near equilibrium. This is accomplished by examining the pitch equilibrium angle at different points in the orbit. These angles are determined for several periods during the mission. The second approach analytically determines a pitch angle so that the buildup of secular momentum over one orbit is minimized. These angles are computed for several periods during the mission.

The general equations of motion for a spacecraft placed in an elliptic orbit, and under the influence of gravity gradient and aerodynamic torques, are given by[10]

$$M\ddot{\Phi} + C\dot{\Phi} + K\Phi + p_0 = P_d[N_0 + N_L L^2 + N_J(\Phi + \Phi^*)] + T_{g0} + T_{ga}\Phi \tag{15}$$

The linearized equilibrium condition is obtained by setting the rates and accelerations of the spacecraft with respect to the rotating attitude axes to zero.

$$\Phi_e = p^{-1}[T_{g0} + P_d(N_0 + N_L L^2) + N_J\Phi^* - p_0] \tag{16}$$

where

$$p = K - T_{ga} - P_d N_J \tag{17}$$

Equation (16) indicates that the equilibrium position depends upon the bias aerodynamic and gravity gradient torques, the effect of super-rotation and p_0 which depends upon the moments of inertia of the spacecraft and the rate of change of the true anomaly and its first and second derivatives. These equations give the instantaneous equilibrium positions under the influence of external torques.

The instantaneous values of the equilibrium pitch angles as a function of the mean anomaly for different periods were obtained by using Eqs. (16) and (17). The true anomaly was approximated from the mean anomaly M by the relation

$$f \simeq M + 2e\sin M + (5/4)e^2\sin 2M \tag{18}$$

The results indicate that the equilibrium angles vary considerably over one orbit. At times large angles were obtained which prevented the drawing of continuous curves. These were obtained for periods during which the pitch angle was difficult to control in flight. It is noted that these large angles violate the linear constraint.

Figures 4 and 5 depict the results of six representative cases. Figure 4 shows the instantaneous value of the pitch angle as a function of the mean anomaly for the Dec. 16, 1979, Jan. 22, 1980, and March 13, 1980 orbits. During this period the attitude dependent gravity gradient torque is greater than the

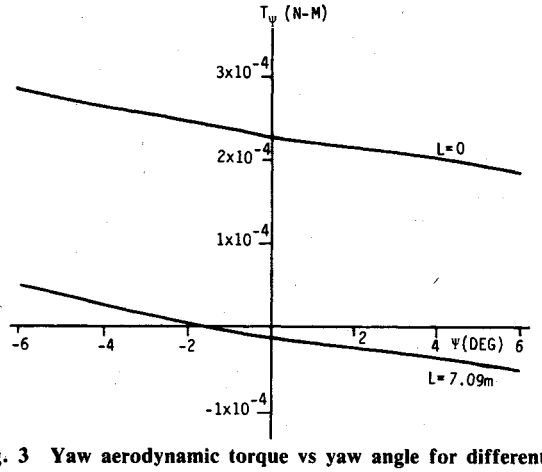

Fig. 3 Yaw aerodynamic torque vs yaw angle for different boom lengths.

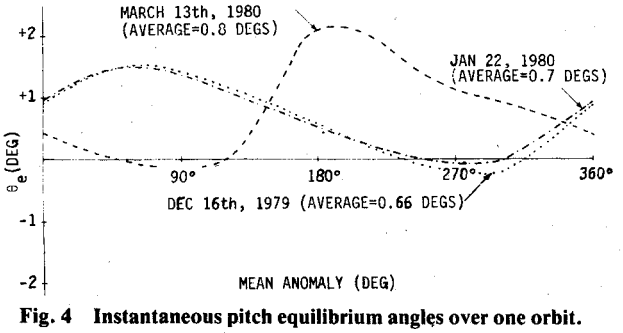

Fig. 4 Instantaneous pitch equilibrium angles over one orbit.

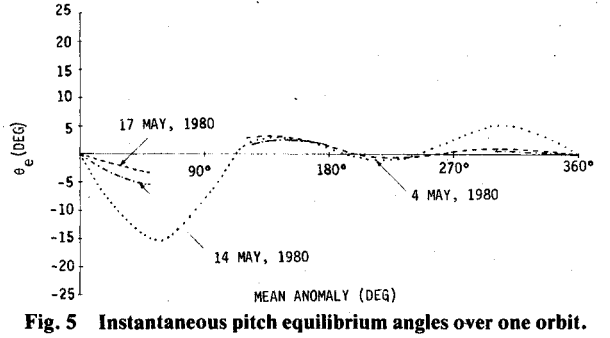

Fig. 5 Instantaneous pitch equilibrium angles over one orbit.

attitude dependent aerodynamic torque. The average pitch equilibrium angle (computed from 24 orbital positions) increased slightly during the period of Dec. 16, 1979 to March 13, 1980. Note that the instantaneous values of the pitch angles vary considerably from the mean value.

Flight data and observations during the flight of Magsat indicated that for a period of about two weeks starting around May 8, 1980, there was no preferred pitch angle at which the spacecraft could be kept without excessive momentum fluctuations. Figure 5 shows the theoretically computed average pitch angle for orbits on May 4, May 14, and May 17, 1980. All orbits show much larger fluctuations in the equilibrium pitch angles. The curves for the May 14 and May 17 orbits are discontinuous as very large values for the equilibrium pitch angle were obtained. Values for average pitch angle are not shown on these curves as they were unrealistic due to one or more very large sample values of the equilibrium pitch angle.

In order to gain further insight, an integral approach is used to determine a pitch angle $\bar{\theta}_e$ at which the secular buildup of angular momentum over one orbit is minimized. The pitch axis dynamics are governed by the equation

$$I_{yy}(\ddot{\theta}-\ddot{f}) = P_d[N_{B2}+N_{J22}(\theta+\theta^*)]$$

$$-3\omega_0^2\frac{(1+3e\cos f)}{(1-e^2)^3}[-I_{xz}+(I_{xx}-I_{zz})\theta] \tag{19}$$

Here, N_{B2} is the contribution of the pitch bias aerodynamic torque and N_{J22} the pitch dependent aerodynamic torque along the pitch axis. In the preceding equation, a small effect of the yaw motion on the pitch motion due to product of inertia effects has been ignored. Since $\ddot{f}$ and θ^* vary periodically over one orbit, an average value of pitch angle $\bar{\theta}$ can be determined at which the gravity gradient and aerodynamic torques over an orbit produce no change in angular momentum. If T is the period of one orbit, the desired condition is given by the equation

$$\int_0^T P_d[N_{B2}+N_{J22}\bar{\theta}_e]$$

$$-3\omega_0^2\frac{(1+3e\cos f)}{(1-e^2)^3}[-I_{xz}+(I_{xx}-I_{zz})\bar{\theta}_e]\,dt=0 \tag{20}$$

Since the peak velocity of the wind is less than 10% of the spacecraft velocity, V_d^2 in the dynamic pressure can be approximated by the square of the spacecraft velocity V_{sc}. A suitable expression for density variation can be obtained by using the relation

$$h=r-r_e=a(1-e^2)/(1+e\cos f)-r_e$$

Here r_e is the Earth's radius.

On expanding the preceding equation in a binomial series, neglecting terms of second and higher order in eccentricity, and substituting the result in Eq. (2), the following equations are obtained.

$$\rho=\rho_0(a)\exp(K_0\cos f) \tag{21}$$

$$\rho_0=k\exp[-(a-r_e)/62]; \qquad K_0=ae/62 \tag{22}$$

Thus, ρ_0 and K_0 are factors that have been introduced for convenience and are a function of the orbit being investigated.

As a first approximation, the angular velocity over an orbit can be assumed to be constant so that Eq. (20) can be integrated over the variable f, the limits being 0-2π. This is a valid assumption since the major variation in the aerodynamic torque is due to variations in the density and not the angular velocity. The integration is accomplished after Eq. (21) is expanded in a series with the variable $K_0\cos f$ and the result substituted in Eq. (20).

The angle $\bar{\theta}_e$ can be shown to be given by the relation

$$\bar{\theta}_e=\frac{\dfrac{6I_{xz}}{\{a(1-e^2)\}^2}+[(1+e^2)K_1+2eK_2]\rho_0N_{B2}}{\dfrac{6(I_{xx}-I_{zz})}{\{a(1-e^2)\}^2}-[(1+e^2)K_1+2eK_2]\rho_0N_{J22}} \tag{23}$$

$$K_1=1+\frac{K_0^2}{4}+\frac{K_0^4}{64}+\ldots \tag{24}$$

$$K_2=\frac{K_0}{2}+\frac{K_0^3}{16}+\ldots \tag{25}$$

It should be noted that though K_0 has values slightly greater than unity in the Magsat flight regime, the series converge.

The values of $\bar{\theta}_e$ as computed from Eq. (23) are plotted in Fig. 6 as a function of mission lifetime. They indicate that the average equilibrium angle increased slightly during the period of Dec. 1979 to March 1980. This trend was also exhibited by the average value of the instantaneous pitch equilibrium angle. They show that the pitch angle $\bar{\theta}_e$ suddenly became more positive and then went to a large negative value. This discontinuity occurred during the period of May 7 to May 21. Flight data and experience indicate that during this period it was not possible to find any pitch angle at which the angular momentum would be stable. This is the period during which the attitude dependent aerodynamic and gravity gradient torques are of the same magnitude and opposite in sign. After this transition period, the equilibrium angle $\bar{\theta}_e$ became negative and then decreased in magnitude. This trend was also seen during flight. Thus, a nonzero equilibrium angle is the result of gravity gradient and aerodynamic bias torques. Of these, the gravity gradient bias torque due to product of inertia effects is the dominant torque during the early part of the mission. The transition period (singularity) occurs when the attitude dependent aerodynamic and gravity dependent torques are of the same magnitude and opposite in sign.

It should be noted that errors in the value of $\bar{\theta}_e$ can arise due to errors in the model. In order to investigate the nature and effect of these errors, a parametric study was conducted. It indicates[10] that errors in the density and aerodynamic stiffness are of more significance than errors in the bias torque.

Roll-Yaw Axis Results

The long-term motion of the spacecraft about the roll-yaw axes is studied by examining the torque-free motion of a spacecraft and assessing the implication of approximating the spacecraft by a gyroscope under the influence of external torques. If the products of inertia are neglected and the spacecraft assumed to be in a circular orbit, it can be shown that the characteristic equation for Eq. (15) is

$$I_{xx}I_{zz}s^4+[I_{xx}\{(I_{yy}-I_{xx})\omega_0-h_w\}\omega_0-I_{zz}\{(I_{zz}-I_{yy})\omega_0$$

$$+h_w\}\omega_0+\{(I_{xx}-I_{yy}+I_{zz})\omega_0+h_w\}^2]s^2$$

$$-\{(I_{zz}-I_{yy})\omega_0+h_w\}+\{(I_{yy}-I_{xx})\omega_0-h_w\}\omega_0^2=0 \tag{26}$$

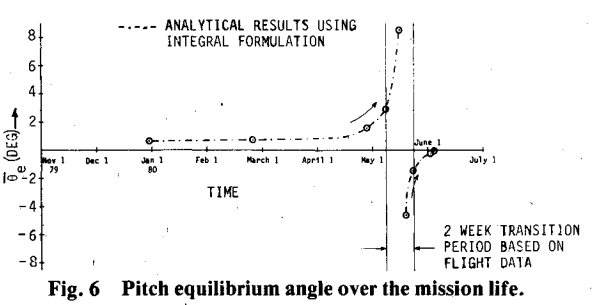

Fig. 6 Pitch equilibrium angle over the mission life.

In order to gain some insight into the nature of Magsat dynamics, the orbital period can be assumed to be 92.26 min. The characteristic frequencies have periods of 153.9 s and 92.10 min. Note that no nutation damping terms are present as the products of inertia are ignored. The short period motion can be identified to be nutation and is ignored in the subsequent analysis. If the difference in period between the long period and the orbital period is ignored, then the equations of motion can be written in a form such that the torque-free motion occurs at the orbital frequency. This, in turn, can be achieved by considering the equations governing the motion of a momentum wheel, under the influence of the external torques. They are given by

$$-h_w(\dot{\psi}+\dot{f}\phi)=T_{g01}+T_{ga11}\phi \tag{27}$$

$$h_w(\dot{\phi}-\dot{f}\psi)=P_d[N_{03}+N_{L3}L^2+N_{J33}(\psi+\psi^*)]+T_{ga31}\phi \tag{28}$$

For numerical results, the gyroscopic bias included the angular momentum due to the orbiting spacecraft. Note that the gravity gradient effects due to products of inertia have been included.

Equation (27) indicates that the roll torque acting on the spacecraft primarily consists of a bias gravity gradient torque due to product of inertia and an attitude dependent gravity gradient torque. The yaw torque represented by Eq. (28) is primarily due to aerodynamic effects. It consists of a boom length dependent bias torque and an attitude dependent torque. There is a small roll dependent gravity gradient yaw torque due to the product of inertia I_{xz}.

If the spacecraft and momentum wheel are regarded as a gyroscope, the negative bias torque due to gravity gradient effects will cause a motion in a negative sense about the yaw axis. Thus, the pitch axis would move in a direction of increasing declination at the ascending node and increasing right ascension at the North Pole. Thus, one of the effects of the bias gravity gradient torque could be expected to be a clockwise motion on the celestial sphere with a frequency of about one orbit. Note that the magnitude of the gravity gradient torque changes very little due to the small eccentricity of the orbit and, thus, this periodic motion would be expected to contribute very little to any long-term drift of the pitch axis.

The effect of the bias yaw torque is reflected in the roll motion at any instant of time. Since the orbit is eccentric, the density varies by a factor of five during the orbit, and as such the bias torque could be expected to cause net drifts whose direction is governed by the direction of roll motion at perigee. This suggests that one control philosophy would be to select a boom length L so that the boom length dependent bias torque, $P_dN_{L3}L^2$, is equal and opposite to the bias torque, P_dN_{03}, with the boom fully retracted. In such a case, the total bias aerodynamic torque about the yaw axis would be zero. The resulting motion would then be the sum of a negligibly small drift caused by the gravity gradient bias torque and attitude dependent gravity gradient and aerodynamic torques.

Analytical Results

The long-term motion of the pitch axis of the spacecraft in a circular orbit is considered. For the case of a circular orbit, it is relatively easy to obtain the closed-form solutions of the pitch axis in terms of the relative right ascension and declination with respect to the negative orbit normal. The combined effects of gravity gradient torque and the aerodynamic torque including the super-rotation of the atmosphere are considered.

Equations (27) and (28) can be expressed in the form

$$\dot{\phi}-(\omega_0-\epsilon_2)\psi+a\phi=\epsilon_2\psi_s\cos\omega_0 t+A \tag{29}$$

$$\dot{\psi}+(\omega_0+\epsilon_1)\phi=G \tag{30}$$

Here

$$\epsilon_1=T_{ga11/hw};\qquad \epsilon_2=P_dN_{J33}/h_w$$

$$G=-T_{g01}/h_w;\qquad A=P_d(N_{03}+N_{L3}L^2)/h_w$$

$$a=T_{ga31}/h_w;\qquad \psi_s=(\omega_a/\omega_0)\sin i$$

Equations (29) and (30) were integrated so that the long-term motion could be expressed in terms of the roll and yaw angles. However, flight experience with Magsat indicates that for a better understanding of the dynamics, the parameters used to describe the motion should be the differences between the right ascension and declination of the pitch axis and the right ascension and declination of the NON, respectively. For small perturbations of the pitch axis from the NON, the roll and yaw angles can be expressed in terms of the relative right ascension (α) and relative declination (δ).

$$\phi=\alpha\cos\beta\sin i-\delta\sin\beta \tag{31}$$

$$\psi=-\alpha\sin\beta\sin i-\delta\cos\beta \tag{32}$$

Here β is the sum of the argument of perigee (D) and the true anomaly.

The solution to the roll-yaw equations of motion can then be expressed in the form

$$\alpha(t)=\frac{e^{-a/2t}}{\sin i}\left[\left\{\phi_0-\left(\frac{G}{\omega_3}\right)\right\}\cos(\omega_3-\omega_0)t+\left\{\psi_0+\left(\frac{A}{\omega_3}\right)+P\omega_3\right\}\sin(\omega_3-\omega_0)t\right]+\frac{1}{\sin i}\left[\left(\frac{G}{\omega_3}\right)\cos\omega_0 t+\left(\frac{A}{\omega_3}\right)\sin\omega_0 t+P\left\{\frac{(\epsilon_1-\epsilon_2)}{4}\right\}\sin 2\omega_0 t\right] \tag{33}$$

$$\delta(t)=e^{-a/2t}[\{\phi_0-(G/\omega_3)\}\sin(\omega_3-\omega_0)t-\{\psi_0+(A/\omega_3)+P\omega_3\}\cos(\omega_3-\omega_0)t]+\delta_f-(G/\omega_3)\sin\omega_0 t+(A/\omega_3)\cos\omega_0 t-P\{(\epsilon_1-\epsilon_2)/4\}\cos 2\omega_0 t \tag{34}$$

where

$$P=\epsilon_2\psi_s/(\omega_3^2-\omega_0^2) \tag{35}$$

$$\delta_f=P\{\omega_0+(\epsilon_1-\epsilon_2)/4\} \tag{36}$$

$$\omega_3=\{(\omega_0+\epsilon_1)(\omega_0-\epsilon_2)\}^{1/2} \tag{37}$$

The total motion consists of a transient part and a steady-state part. The transient part decays with a time period of $2/a$. This decay is due to the bias gravity gradient torque which in turn is due to the product of inertia. The direction of motion is controlled by the sign of $(\omega_3-\omega_0)$ and is counterclockwise for the mass and aerodynamic characteristics of Magsat. If the aerodynamic bias torque and, hence, A is zero, this motion can be suppressed by allowing $\phi_0=G/\omega_3$ and $\psi_0=-P\omega_3$.

The steady-state solution consists of a motion at the orbital frequency and twice the orbital frequency. The motion at the orbital frequency is caused by bias aerodynamic and gravity gradient torques. The motion at twice the orbital frequency is negligibly small in magnitude. The equations show that the center of the pitch axis motion is offset along the declination by the angle δ_f. This offset is not equal to the super-rotation angle.

Simulation Results

A survey was made over the entire mission life of periods during which the pitch axis appeared to drift in the vicinity of

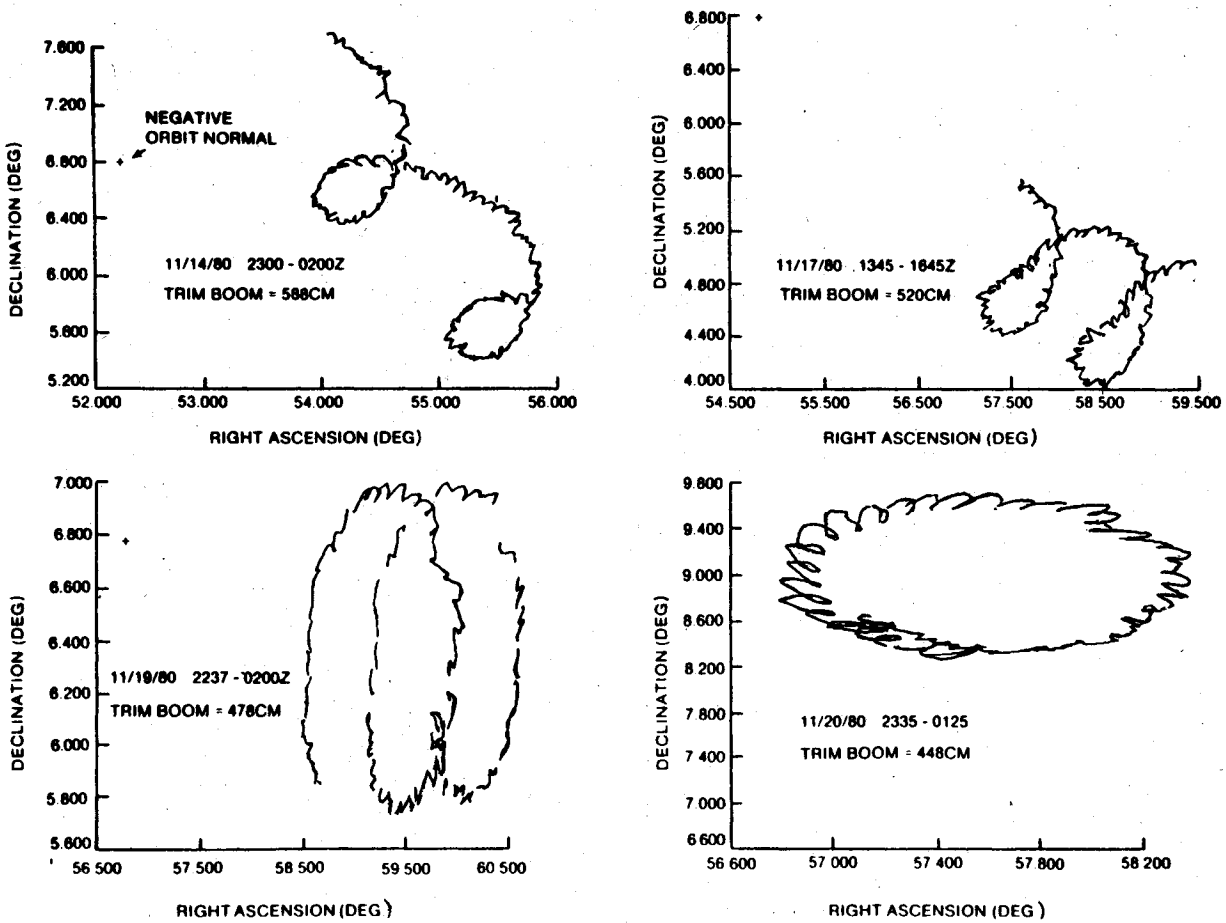

Fig. 7 Pitch axis drift for four boom lengths (flight data[7]).

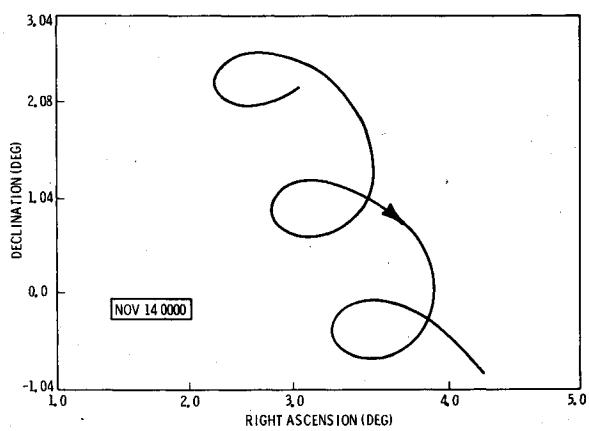

Fig. 8 Pitch axis motion with boom extended beyond trim length (simulation).

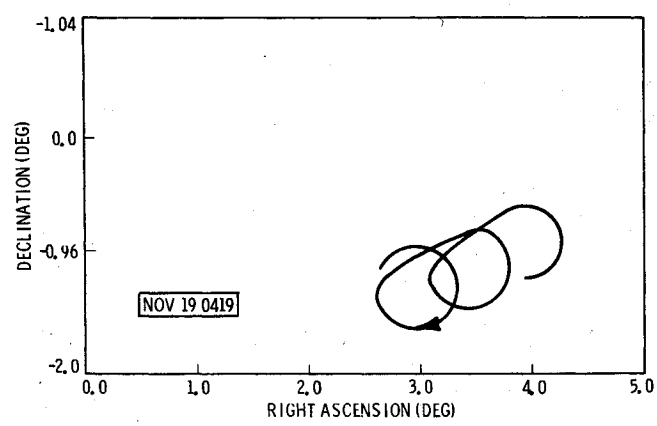

Fig. 9 Pitch axis motion with boom at trim length (simulation).

a point. The survey indicated that the boom length during such periods was in the vicinity of 4.7 m. Thus, it was hypothesized that the bias aerodynamic torque was zero when the boom length was in the vicinity of 4.7 m. The simulation studies were designed to validate the observation that there is no bias torque at a boom length of about 4.7 m and that a control philosophy can be developed as a result of which the drift can be minimized by keeping the boom length at about 4.7 m. The results of the simulation runs are corroborated with flight data.

The orbital drift of the pitch axis, as obtained from flight data[7] is depicted in Fig. 7. It shows the motion of the Magsat spacecraft over several orbits while the boom was being retracted. Figures 8 and 9 were obtained from simulations. In Fig. 8, the boom is extended about 180 cm from the hypothesized trim length of 4.7 m. Though this value is greater than that in flight it was chosen to exaggerate the effect of extending the trim boom beyond the trim length. The nature of the motion compares very favorably with that seen in the top left part of Fig. 7. Figure 9 was obtained with the boom length extended about 9 cm beyond the trim length. This corresponds to the bottom left part of Fig. 7 in which there is a negligible drift in declination and the right ascension increases. Figure 9 shows a similar overlapping motion with increasing right ascension and a small increase in declination.

Figure 10 shows that the motion of the pitch axis over five days remains bounded if the initial attitude is near the apparent trim point. The same set of orbital elements on Jan.

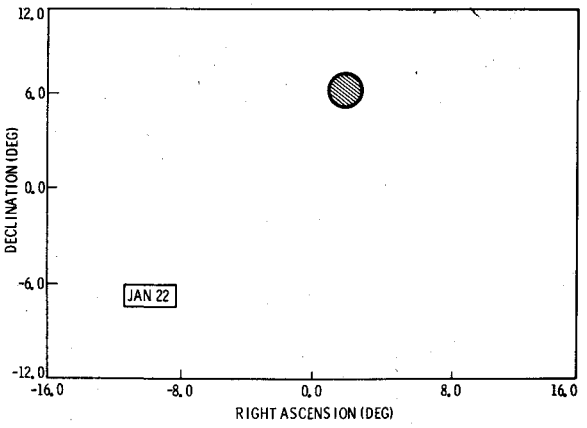

Fig. 10 Initial attitude at trim point and boom at trim length (simulation).

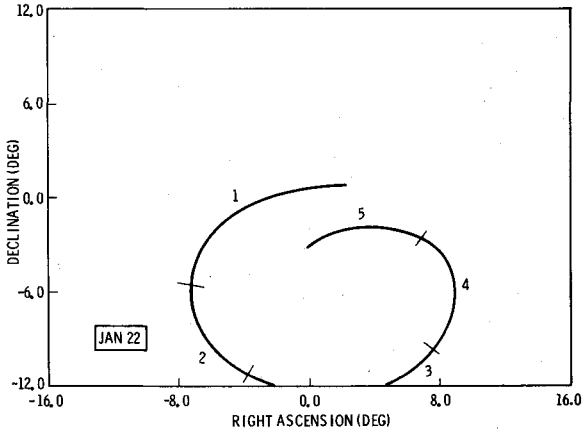

Fig. 11 Pitch axis motion with boom extended beyond trim length (simulation).

22, 1980 was used to generate Fig. 11. The trim boom was extended 1.3 m beyond the trim length. It shows that there is no tendency for the pitch axis to move toward the trim point. The numbers on the curve correspond to the day number from the start of simulation. It should be noted that simulations and flight data indicate that the aerodynamic bias is zero when the trim boom length is 4.7 m. However, the theoretical value of the aerodynamic torque at two different boom lengths and the assumed parabolic distribution suggest that the trim length should be 5.7 m.

Conclusions

The nature of the roll-yaw motion observed during flight can be predicted, simulated, and explained. If the motion due to nutation is neglected, the motion of the pitch axis occurs at three frequencies. A small clockwise motion occurs at a frequency close to the orbital frequency. The magnitude of this motion depends upon the initial attitude at the ascending node, and the bias gravity gradient and aerodynamic torques. A large, counterclockwise elliptical motion can be attributed to the difference in the orbital frequency and the frequency of the spacecraft's roll-yaw motion under the influence of gravity gradient and aerodynamic torques. The effect of the aerodynamic bias torque on this motion and the condition under which this can be eliminated has been derived. The elliptical nature can be attributed partly to the inclination of the orbit. It is shown that for spacecraft with other mass and aerodynamic characteristics, this motion can be clockwise. The period of this motion is of the order of a few days and for a circular orbit has been shown to decrease with increasing density at lower altitudes. The amplitude of the motion does not govern the period of the motion. This supports the observation that the arc length traversed across the celestial sphere was greater when the initial attitude was further from the trim point. A negligibly small component of the motion occurs at twice the orbital frequency. Another hypothesized motion with a period of several weeks was not observed and can not be justified based on the understanding achieved by this study.

Analysis and simulations conducted during the study indicate that a viable control philosophy would be one in which the boom length was kept at a constant trim position of about 4.7 m. If the attitude of the spacecraft is near the trim point, which was of the order of 6 deg above the negative orbit normal, spacecraft drift would be minimal for extended periods of time. Note that according to this control philosophy, the aerodynamic boom would be trimmed when the bias aerodynamic yaw torque on the spacecraft was zero. This approach is in contrast to another hypothesized control philosophy according to which drift could be minimized by "trimming" the aerodynamic boom so that external torques can be balanced at perigee. Its implication is that proper trim point placement rather than occasional trim boom operations (following an initial deployment) is a better approach to drift minimization. Due to the nature of control torques (magnetic torques) on Magsat, preferred directional control of the pitch axis about the trim point is not possible. Some degree of directional control may be possible with the realization that if the aerodynamic boom is greatly extended or retracted from the trim position, the resulting motion would be generally in the direction of roll at perigee. The timing of this motion with the location of the pitch axis during the four to five day elliptical motion yields a certain degree of preferred directional control so that the spacecraft attitude might be maneuvered closer to the trim point.

Day to day variations and uncertainties in atmospheric properties would seem to discourage the prediction of the optimum bias for the pitch angle. The results obtained from an integral approach show a surprisingly excellent correlation with flight data. The model also aids in explaining the different phenomenon observed in the bias pitch angle history.

Acknowledgments

Most of this work was supported by the NASA Goddard Space Flight Center under Contract NAS5-26186. The authors are extremely grateful to Thomas Stengle, Technical Officer, both for providing the flight data and for his helpful comments. Special thanks to P.E. Powell and S. Hendry in obtaining some of the simulation results. Most of this work was performed while the authors were at the OAO Corporation, Greenbelt, Md. The first author thanks Joseph Elko, Manager of Spacecraft Engineering at RCA American Communications, Inc. for his encouragement and support in completion of this paper.

References

[1] Nurre, G.S., "Effects of Aerodynamic Torque on an Asymmetric, Gravity-Stabilized Satellite," *Journal of Spacecraft and Rockets,* Vol. 5, Sept. 1968, pp. 1046-1050.

[2] Sperling, H.J., "Effect of Gravitational and Aerodynamic Torques on a Rigid Skylab-Type Satellite," NASA TMX-64865, June 1, 1974.

[3] Meirovitch, L. and Wallace, F.B., "On the Effect of Aerodynamic and Gravity Gradient Torques on the Attitude Stability of Satellites," *AIAA Journal,* Vol. 4, Dec. 1966, pp. 2196-2202.

[4] Buchanan, H.J., Hopkins, M.S., and Galaboff, Z.J., "Uncontrolled Dynamics of the Skylab Vehicle," *Journal of Guidance and Control,* Vol. 4, May-June 1981, pp. 277-283.

[5] "Magsat Spacecraft Description," Applied Physics Laboratory, Johns Hopkins University, APL Rept. SDO 5146, March 1979.

[6]Tossman, B.E., Mobley, F.F., Fountain, G.H., Heffernan, K.J., Ray, J.C., and Williams, C.E., "Magsat Attitude Control System Design and Performance," *Proceedings of AIAA Guidance and Control Conference,* Danvers, Mass., Paper AIAA-80-1730, Aug. 1980, pp. 95-104.

[7]Stengle, T., "Magsat Attitude Dynamics and Control: Some Observations and Explanations," NASA/Goddard Space Flight Center, Greenbelt, Md., NASA CP-2152, Oct. 1980, pp. 22.1-22.30.

[8]King-Hele, H.G., "A View of Earth and Air," *Philosophical Transactions of the Royal Society of London,* V-278, No. 1277, March 1975, pp. 67-109.

[9]Jacchia, L.G., "Thermospheric Temperature, Density, and Composition: New Models," Smithsonian Astrophysical Observatory, Special Rept. 375, March 1977.

[10]"Spacecraft Dynamics Evalaution of Existing and Future Missions, Vol. I," OAO Corporation, Beltsville, Md., OAOCO Rept. OAO/TR-81/005, Jan. 1981.